Electric Power Systems Research 190 (2021) 106728

Contents lists available at ScienceDirect

Electric Power Systems Research

journal homepage: www.elsevier.com/locate/epsr

Voltage stability support offered by active distribution networks

Giorgos Prionistis*, Theodoros Souxes, Costas Vournas

School of Electrical and Computer Engineering, National Technical University of Athens, Greece

ARTICLE INFO

Keywords:
Active distribution networks
Decentralized control
Maximum power transfer
Reactive support
Voltage stability

ABSTRACT

This paper investigates distributed control schemes with which an Active Distribution Network can help to increase the voltage stability loadability limit of a bulk power system. Active distribution networks with converter connected renewable energy units can improve network operation through their control and regulation resources. In this paper the aim is to enhance power system voltage stability through distributed controls, respecting at the same time the operational limits of the distribution grid. Case studies of a radial power system, as well as of a real power system snapshot are included.

1. Introduction

Dispersed Generation (DG) units operating at distribution level are supplying an increasingly large percentage of load demand [1]. The increased penetration of DG in distribution networks is giving rise to new operational problems due to the reduction of net load (load minus DG), which results in many hours of light net load during day time. This may result in steady-state over voltages both in Distribution and Transmission Systems, during operation with increased dispersed generation. At the same time, the increased DG penetration opens up new opportunities in terms of the network operation optimization and ancillary services provision, such as power loss minimization and voltage and frequency regulation [2], as well as offering emergency support to the bulk power system [3].

The above-mentioned service opportunities are based on the controllability and fast response that Inverter-Based Generators (IBG) can offer. In this paper we consider an Active Distribution Network (ADN), which consists of a number of distribution feeders whose resources can be coordinated by a local feeder controller able to exchange information with a control center (centralized controller). The local feeder resources considered include the Load Tap Changers (LTC) of the distribution transformer, reactive compensation (if present), DG active and reactive power controllers, and possibly energy storage.

In our approach the ADN will be requested to support the transmission network during stressed operation conditions. Various applications have been proposed, aiming at supporting power system stability using distributed generation [4]. The effect of a Wind Farm connected to the Transmission System through a dedicated distribution feeder in providing voltage stability support has been examined in [3]. In [5, 6] a control scheme able to regulate the active and reactive power exchange between transmission and distribution system is presented.

Several other recent papers deal with aspects of distributed and decentralized control of voltage stability involving the distribution network. In [7] (and references therein) the voltage stability limit of a distribution network is examined. However, in practice such limit is not likely to exist in a real distribution feeder, which is designed to avoid excessive voltage drop under maximum permissible loading, while DG will contribute in voltage rise instead of drop. Thus, in this paper we only use the voltage constraints of the distribution feeder and focus on voltage stability of the bulk transmission system.

Reference [8] correctly focuses on the effect DG can have on Voltage Stability of the transmission system including two aspects: voltage control capability of DG, and risk of massive loss of DG due to low voltage. However, a key element determining the interaction between transmission and distribution grid is missing, namely the control of distribution voltage by the bulk power delivery transformer Load Tap Changer (LTC). In this paper we investigate the effect of voltage/reactive control of DGs to offer support to the bulk transmission system in case of emergency, in coordination also with LTC control. On the other hand, the problem of low voltages in the feeder occurring after the LTC and DGs have exhausted their control range is not addressed and is left for future research.

Regarding distribution system control and optimization, a lot of research has been done lately. Reference [9] proposes a distributed optimization involving converter connected DG to maintain voltages within a feeder. The control is based on sensitivity calculations and takes into account converter P and Q limits. In [10], a local optimal reactive power control is proposed, focusing on PV inverters. The work proposes a method to define the optimal Q(P) curve in order to mitigate overvoltages throughout a whole year using minimal reactive power.

* Corresponding author.
E-mail addresses: gprionistis@power.ece.ntua.gr (G. Prionistis), vournas@power.ece.ntua.gr (C. Vournas).

https://doi.org/10.1016/j.epsr.2020.106728
Received 8 October 2019; Received in revised form 19 April 2020; Accepted 2 August 2020
Available online 24 August 2020

The authors of [11] address a centralized probabilistic optimization of the controllers' settings in a distribution grid using gaussian variables to represent node voltages and DG's to find the optimal parameters.

In this paper we take a further step with respect to above mentioned papers, by intentionally varying feeder voltages within the permissible operational limits (for instance in the range ± 5% of nominal), as is typically done for Conservation Voltage Reduction [12]. Thus, a first problem solved in this paper is to determine the full available range of P and Q power injections at the point of connection, while respecting the permissible voltage limits within the feeder.

Following this step, this paper considers distributed control schemes involving ADN that offer an increase of the transmission system voltage stability and loadability margin. Control schemes assume an upper-level controller for the transmission network (typically at the Control Center, part of the Energy Management System) and a lower-level, local controller for each ADN feeder. Minimal communication exchange is assumed between the two levels, as will be further discussed in the relevant Section.

The paper is organized as follows. In Section II, the two-level control approach is presented. Section III explains how the margin sensitivities are obtained from the Voltage Security Assessment (VSA) in the upper level controller. In Section IV, the ADN constraints are presented and Section V describes the control implementation scheme. Section VI includes simulations on a small radial transmission system connected to an 11-bus Medium-Voltage (MV) distribution feeder while Section VII includes a case study implementing the proposed approach on the Hellenic Interconnected System. Section VIII forms the conclusions.

2. Two level control approach

A typical schematic of the two-levels of controls is shown in Fig. 1. The central controller is solving the VSA problem at the Energy Management System (EMS) level, which determines the most constraining contingency and the respective loading margin of the system considering a specific stress direction [13,14]. Based on this computation the sensitivity coefficients of the resulting maximum power transfer (loadability limit) with respect to the power flow exchange at the point of common coupling (PCC) of each ADN feeder are calculated at no extra computational cost and can be sent back to the distributed controller with a very short transmission delay as they consist of a few bytes and do not require a large bandwidth

The local distribution network controller runs a local optimization algorithm, in order to compute the achievable range active and reactive power injection to the transmission system at the PCC with the aid of the available controls, while respecting local constraints. Given the small size of the distribution feeder, the computational time requirement for solving this optimization problem is very small (typically in the order of a second). The information on P and Q injection can be exchanged with the centralized controller and/or can be used used locally. Based on the implementation either the central controller can

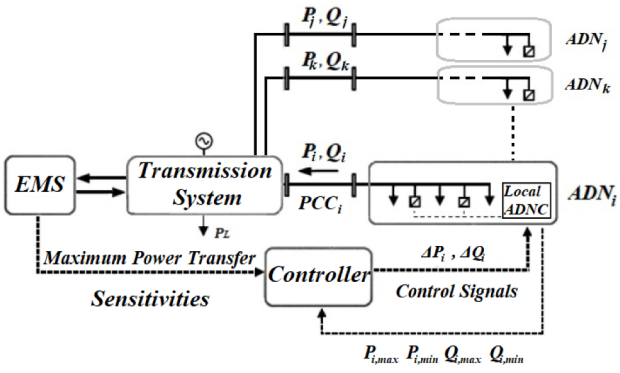

Fig. 1. Concept of ADN Controller and its Interactions.

maximize voltage stability margin by specifying the injections by each ADN feeder and send setpoints control signals P_{ref} and Q_{ref} to the ADN controllers, or each distributed controller adjusts independently its input using the loading margin sensitivity information received by the central controller.

The control variables with which the ADN local controller can achieve the required injections are the voltage and reactive power injection of the inverter-based DG, shunt capacitors, energy storage active power controllers, as well as the setpoint of the LTC of the distribution transformer.

As shown in Fig. 1, the transmission system exchanges power with multiple ADN feeders. A local controller is assumed for each feeder.

The local controller regulates the distribution network so as to respect voltage constraints with minimum effort during operation. However, when receiving an emergency signal (e.g. when the primary transmission voltage drops below a threshold) the control aims to support transmission system voltage stability by increasing the loadability margin as discussed above.

The proposed control approach keeps communication between the transmission system operator and each distribution system to a minimum, since very few data are exchanged every few seconds. It also avoids the analysis of the combined transmission and distribution system, as it is not practical to access the detailed configuration of every distribution feeder. Thus, the control schemes proposed decouples the two systems, solving the optimization problem for each system separately.

3. Loadability margin and its sensitivities

The voltage stability, or loadability limit is associated with maximum power transfer in a power system [14]. The resulting most constraining loadability limit is notated as P_{max}. There are several methods with which this limit and the associated voltage stability margin can be computed, which will not be discussed in this paper. In all cases for a correct determination of the limit power system long-term equilibrium equations must be satisfied:

$$f(\mathbf{x}, \mathbf{p}) = 0 \tag{1}$$

where vector $\boldsymbol{x}$ contains the n state and algebraic variables, $\boldsymbol{p}$ is a vector of load parameters (typically active, as well as reactive demands) and $\boldsymbol{f}$ is a vector of smooth functions. Note that these include, but are not limited to the power flow equations [13].

To obtain the voltage stability margin a direction of stress has to be defined. This corresponds to a direction vector in load parameter space denoted as d:

$$p = p_o + S\mathbf{d} \tag{2}$$

where S is a scalar and it is assumed that $\boldsymbol{d}$ is such that S corresponds to the total active load increase (d_i elements corresponding to load active power add up to 1). With this notation the voltage stability margin is the solution of the following problem:

$$\begin{aligned} &\max_{S,x} S \\ &subject\ to\ \ f(x,\ p)\ =\ 0 \end{aligned} \tag{3}$$

with $\boldsymbol{p}$ as in (2).

At the solution of the optimization problem, the Jacobian f_x of the equilibrium equations is proven to be singular [13], thus it has a zero eigenvalue and the corresponding left eigenvector $\mathbf{w}$ is the vector of Lagrange multipliers of the optimization problem. The solution of (3) corresponds to the VSM S_{max}. As stated above, the corresponding total load is denoted as P_{max}. The Lagrange multipliers determine the sensitivities of P_{max} to the change of power injection at each bus. We note as w_p, w_q the multipliers corresponding to active and reactive injection at each ADN feeder connection bus.

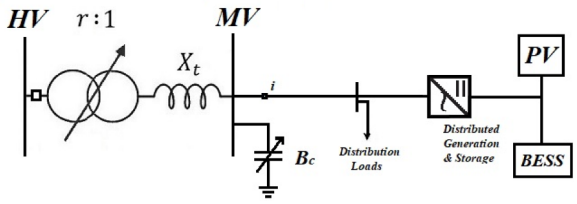

Fig. 2. One-line diagram of typical active distribution network consisting of multiple MV feeders.

4. Distribution feeder constraints

The one-line diagram of a typical active distribution network feeder is presented in Fig. 2.

The local ADN controller is assumed to be able to communicate with the devices and take appropriate control actions to accomplish the following tasks:

- Monitor and regulate the distribution network voltages in order to ensure that operational limits are respected.
- Contribute to voltage stability support when required by the EMS, or when the HV voltage falls below a specified threshold.

It is noted at this point that this paper deals with long-term voltage stability and how this can be supported by the ADN. Thus fast (short-term) response of controllers is not considered in detail. It is just assumed that all control loops are stable and the required response (e.g. voltage regulation) is obtained practically instantaneously with respect to long-term dynamics.

For any given load demand and DG production, the operational constraints for the distribution feeder are the following.

$$\begin{aligned} &V_{min} \le V_j \le V_{max}\ ,\ j = 1. .N \\ &I_{jk} < I_{max,jk}\ ,\ j,k = 1. .N \\ &Q_{PV\,min} \le Q_{PV\,j} \le Q_{PV\,max}\ ,\ j = 1. .N \\ &r_{min} \le r \le r_{max} \end{aligned} \tag{4}$$

where V_j is the voltage for the j-th bus of the distribution network, I_{jk} is the line current between buses j and k, and Q_{PVj} is the reactive power produced by the DG located on bus j, and its limits are shown in the capability curve of Fig. 3. Limiting values $Q_{PV,min}$, $Q_{PV,max}$ can be expressed as follows:

$$Q_{PV\{max,min\}} = \pm\sqrt{(V_j I_{PV,max})^2 - P_{PV}^2} \tag{5}$$

The capability curve is shown in Fig. 3 for constant voltage (PQ-diagram).

As mentioned before, the local distribution feeder controller is essential to make the feeder part of an active distribution network.

The available controls in an active distribution feeder include:

- Switched Shunt Capacitors
- HV/MV transformer Load Tap Changer (LTC)
- Photovoltaics (PVs) or other forms of IBG
- Battery Energy Storage Systems (BESS)

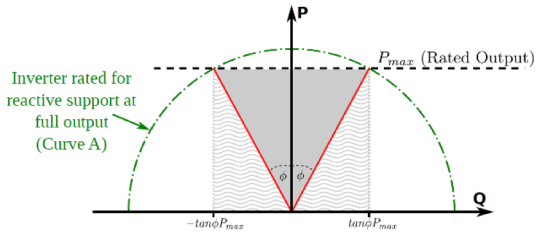

Fig. 3. Inverter PQ-diagram under constant voltage.

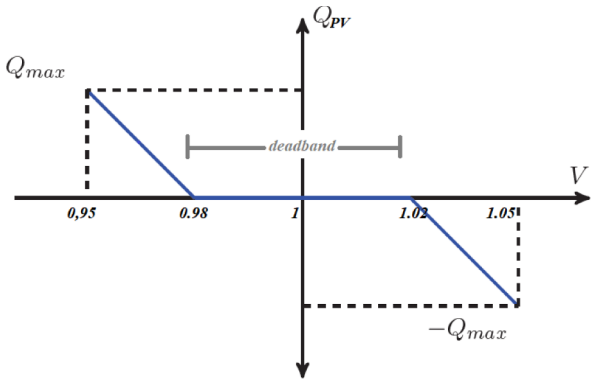

Fig. 4. Q(V) control curve.

In particular, the LTC control variable considered is the voltage setpoint of the medium voltage bus, whose voltage at equilibrium is:

$$V_{LTC,set} - d \le V_{MV} \le V_{LTC,set} + d \tag{6}$$

where d is half the dead band and V_{MV} is the voltage of the secondary bus of the transformer.

Another control variable considered in this paper is the voltage reference of the bus where each DG is connected, assuming the converter allows for tight voltage control. In general, converters above certain capacity are required to have reactive power capabilities. In this study, three cases for the IBG reactive control are considered: Unity Power Factor (UPF), operation according to the Q(V) characteristic shown in Fig. 4 and Constant (tight) Voltage Control (CVC). In the first two cases (UPF and QV characteristic) the ADN controller sets the LTC setpoint as to avoid any voltage violation along the feeder. In the third case it can also specify the voltage at PV connection points making the control problem multi-variable.

5. Load margin control implementation

The proposed distributed control scheme can be implemented using two different coordination algorithms: a distributed optimization scheme based on the sensitivity factors provided by the EMS, or a centralized optimization based on PQ injection range specified by the ADN controllers. The advantage of the first scheme is that it does not require a change in existing voltage stability margin running at the EMS level, while the second scheme requires a new implementation of an optimization solver.

5.1. Distributed optimization scheme

The first step of this scheme is the solution of the Voltage Stability Margin problem at the EMS level and the determination of P_{max} and its sensitivity coefficients w_p and w_q. Each local controller is then solving a linearized maximization problem using a gradient control, subject to the constraints (4).

The objective function for the distributed optimization problem is created using the sensitivities provided:

$$\begin{aligned} &\max_{u_1,\ ..,u_n} \Delta P_{max} = w_p \Delta P_i(u_1, ..,u_n) + \\ &w_q \Delta Q_i(u_1, ..,u_n) \end{aligned} \tag{7}$$

where $\boldsymbol{u}$ represents the control variables and ΔP_i, ΔQ_i, are the added active and reactive injections at the PCC of the i-th distribution feeder. The control vector includes the LTC setpoint and the PV voltages in case of tight voltage control.

$$\boldsymbol{u} = \left[V_{LTC,set},\ V_{PV_j}\right] \tag{8}$$

This process is inherently iterative, as the Voltage Stability problem can be solved again after the distributed control is implemented and

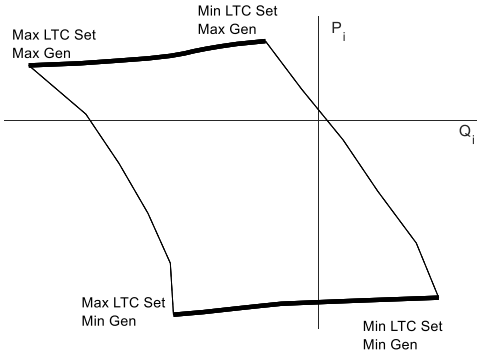

Fig. 5. Feeder power injection capability graph.

new sensitivities can be calculated. The loop closes when the control variables can no longer increase the Maximum Power Transfer without violating the operational limits of the distribution feeder.

5.2. Central control with distributed actuation

In this scheme the first step is taken by the ADN controllers, which provide an estimation of the active and reactive power injection limits of each feeder. The available range in the PQ space is transmitted to the central controller and the voltage stability margin maximization problem is solved centrally with P_i and Q_i as control variables within their available range thus providing P and Q setpoints to be sent back to each distributed controller.

Fig. 5 presents the available power injection that is created by altering the Voltage Setpoint of the LTC and the Active Power Generation of the PVs from minimum to maximum. This graph can be computed either by solving an optimization problem for various values of DG production, or using repeated load flow solutions. Due to the small size of the feeder this calculation can be performed in reasonable time.

6. Test feeder and radial transmission system

The proposed control scheme is initially tested in a radial 12-bus, 20kV distribution feeder connected to the middle of a high voltage 150kV (HV) transmission corridor through an HV/MV transformer equipped with Load Tap Changer (LTC). The test feeder corresponds to an overhead distribution line with total length of 22km and conductor type ACSR-95. For the sake of simplicity, a single feeder is considered in this example. The control scheme will be the same for multiple feeders in a substation, since the values of interest would still be the injections into the transmission system.

The five loads connected to the feeder are modelled transiently (in the short-term) as constant impedance loads. Load restoration in the long-term is indirectly achieved through the operation of the LTC, which restores MV voltage and thus load consumption. The three Photovoltaic (PV) units are modelled as converter connected generators. The test feeder topology is shown in Fig. 6 with data listed in Table 1.

The first step is to give an example of the calculation of active and

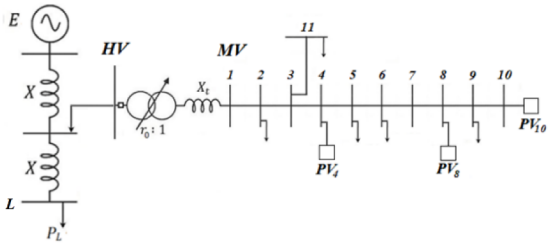

Fig. 6. Test feeder and transmission line.

Table 1
Line data in per unit for system base 50 MVA.

Bus		*R*	*X*	*B*
1	2	0.0672	0.1044	0.0000011
2	3	0.0430	0.0668	0.0000007
3	4	0.0306	0.0476	0.0000005
4	5	0.0726	0.1127	0.0000012
5	6	0.0124	0.0192	0.0000002
6	7	0.1344	0.2088	0.0000021
7	8	0.1357	0.2108	0.0000022
8	9	0.0376	0.0585	0.0000006
9	10	0.0403	0.0626	0.0000006
3	11	0.0306	0.0476	0.0000005

reactive power injection capability as in Section V.B, for P_i and Q_i injected to the transmission HV bus of the substation, while respecting the operational limits set for the distribution feeder.

Each PV has a rating of 5.5 MVA, with a maximum active power of 5 MW, while the total load of the feeder is 10.82 MW and 2.64 MVar.

The minimum and maximum values for the LTC voltage setpoint for which all bus voltages are within limits are calculated for PV operation at maximum and minimum power generation, assuming either UPF or Q(V) control and are presented in Table 2.

The PQ injection capability for the test feeder is calculated and shown in Fig. 7. As seen, the limits depend on the assumption concerning the control of DG. The letters in Table 2 refer to the corresponding points on the graph. For unity power factor the Q limits are obviously limited. The P limits assume the presence of battery energy storage at each PV bus, so that the desired P can be generated at will.

The control scheme for this simple system provides exactly the same solution using either Scheme A or Scheme B of the previous Section V. In all cases the optimum (maximum transfer capability or maximum voltage stability margin) is obtained for the upper right corner of the graph of Fig. 7 marked as point B (B'). In Table 3, the increase in the Maximum Power Transfer for each control case is shown. The stability margin increase obtained by the feeder controls is small (1 to 4MW), but compared to the overall rating of the PV units (16.5 MVA) represent a percentage from 6% to 24%, which is not negligible.

If no battery storage is available, then the capability graph reduces to a single curve corresponding to the P injection by the PVs. Assuming a maximum generation of 2 MW for each PV unit, the results of Table 4 are obtained for different DG converter reactive power controls (UPF, Q (V), or tight V control).

The results are also validated using simulation, in which the load conductance is increased with a constant rate while the feeder controls are active. At first DGs are assumed to operate under Unity Power Factor. When the voltage of the HV bus drops below 0.90 p.u. the local feeder controller lowers the LTC setpoint to 0.95 and changes the operation of the PVs into Q(V) control or Constant Voltage Control respectively.

Following the simulation, the consumed load active power is plotted versus load voltage in a P-V curve as shown in Fig. 8. Both load consumption and voltage plotted refer to the load bus L of the radial transmission system of Fig. 6. A different curve is plotted for each type of DG reactive power control shown in Fig. 8 with a different color. These curves clearly indicate the increase of maximum load power delivered which is the same shown in Table 3.

Table 2
LTC voltage setpoint for different cases.

	UPF		*Q(V)*	
	$V_{LTC,set\|max}$	$V_{LTC,set\|min}$	$V_{LTC,set\|max}$	$V_{LTC,set\|min}$
max PV Generation	1.03 (A')	0.95 (B')	1.05 (A)	0.95 (B)
Min PV Generation	1.05 (C')	1.03 (D')	1.05 (C)	0.97 (D)

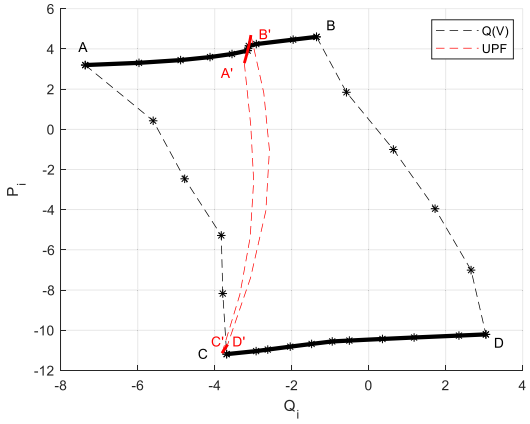

Fig. 7. Test feeder PQ injection capability limits.

Table 3
Maximum power transfer for different controls.

Control	P_i *(MW)*	Q_i *(MVar)*	w_p	w_q	P_{max} *(MW)*
UPF	4.689	-3.017	0.1933	0.6046	136.94
Q(V)	4.599	-1.357	0.1936	0.6024	137.95
CVC	3.786	3.916	0.1956	0.5957	140.95

Table 4
Power injections for generation of 2 MW per PV.

	UPF		Q(V)		CVC	
LTC_{set}	P_i *(MW)*	Q_i *(MVar)*	P_i *(MW)*	Q_i *(MVar)*	P_i *(MW)*	Q_i *(MVar)*
0.95	-	-	-3.9789	1.6708	-4.6682	5.8101
0.96	-	-	-4.0534	0.8752	-4.6172	4.1976
0.97	-	-	-4.1365	0.0446	-4.6845	4.0320
0.98	-	-	-4.2287	-0.8234	-4.7647	3.8245
0.99	-4.1318	-2.6801	-4.2784	-1.2717	-4.8576	3.5718
1	-4.2542	-2.7167	-4.3306	-1.7299	-4.8316	1.6766
1.01	-4.3789	-2.7540	-4.4705	-2.3171	-4.8268	0.6942
1.02	-4.6357	-2.8132	-4.5461	-2.5991	-4.8344	-1.3432
1.03	-4.7679	-2.8711	-4.7689	-2.8709	-4.8662	-3.4820
1.04	-5.0403	-2.9536	-5.0404	-2.9534	-4.9244	-5.7278
1.05	-5.1807	-2.9963	-5.1614	-3.1742	-5.0570	-6.4153

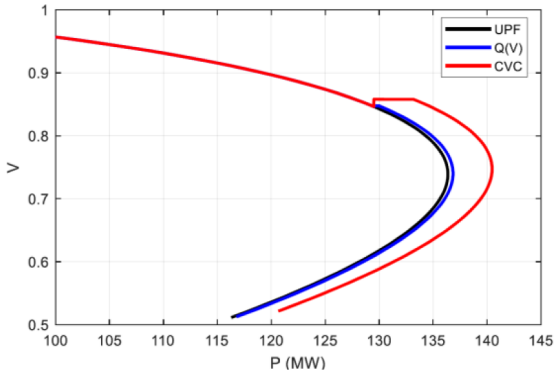

Fig. 8. P-V curve (Nose Curve) for each case.

7. Application to the Hellenic interconnected system

7.1. Operating point and method of analysis

The distributed control scheme proposed is implemented in this Section to a real system to demonstrate active distribution network support to the transmission system in a realistic scenario.

The examined system is the Hellenic Interconnected System and more specifically a specific snapshot of June 2010, for which the on-line VSA operating at the Control Center [15] identified a critical contingency for which the system was insecure, meaning that if the contingency happened, a voltage collapse would result. The most affected area for this contingency was the Peloponnese region in the South of the System. The critical contingency was the loss of a synchronous generator unit in the area as explained in detail in [15].

Contrary to the single load, radial transmission system considered in the previous Section, in a real, meshed power system, maximum power conditions can occur in one corridor, or in one area, before the advent of voltage instability. In this study, we monitor voltage instability occurrence through long-term sensitivity and eigenvalue computation [13]. At this point the left eigenvalue of the almost zero eigenvalue of the long- term Jacobian is calculated and the corresponding elements of Lagrange multipliers of P and Q injections at each bus are recorded.

The whole Hellenic System is simulated using WPSTAB software [15] considering the critical generating unit disconnection after 100s of simulation time. Then a uniform load demand increase is simulated to stress the system beyond its voltage stability limit. The demand increase is the same for all voltage stability support schemes considered in this paper. The generating units gradually reach their overexcitation limits and the resulting low voltage eventually causes a succession of generating unit undervoltage trips, so that the system eventually collapses.

Fig. 9 is the so-called regional PV curve, which shows the total consumed active load in Peloponnese against the voltage of a characteristic bus of the area. It is noted that the maximum of this curve is not strictly a voltage stability limit in a multiple load system, but it still represents the maximum load recovery possible in the area. In the following we will use this as an estimation of maximum load consumption in Peloponnese following the insecure contingency. In this sense it is evident that the maximum possible consumption (841.5 MW) is less than the pre-disturbance value (862.9 MW), which is indicative of voltage instability if load tries to restore its initial consumption.

In Fig. 10, the simulated bus voltages of two buses are shown as a function of simulation time for the considered unstable contingency.

7.2. Voltage stability support scheme

The Lagrange multipliers calculated as described above are given as input to a number of feeders added to the transmission system model and a distributed ADN control as in Section V.A is assumed at each of them.

For all the buses the same test feeder of Fig. 6 is used, scaled accordingly in order to maintain the same initial condition of the bulk power system. It is noted that this means that roughly 60% of the feeder load is supplied by the PVs so that the actual feeder load is roughly 2.5 times larger than that measured at the transmission bus. It is not unreasonable to consider that this can be the case for some distribution feeders during summer, but detailed information for each feeder have

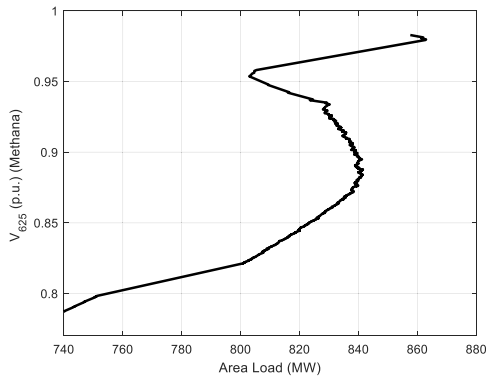

Fig. 9. P-V curve (Nose Curve) for the Peloponnesian bus of Methana.

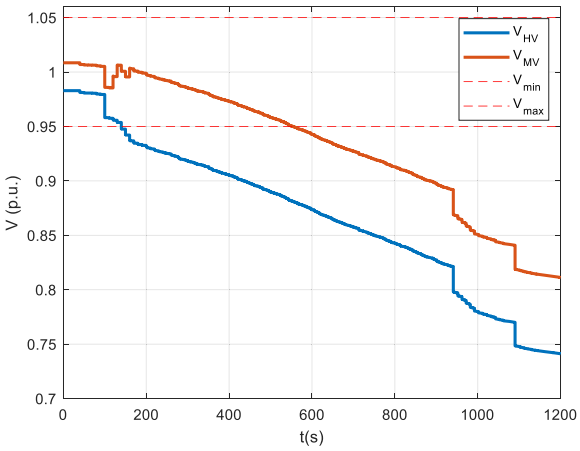

Fig. 10. Bus voltages for HV Bus 625 and MV Bus 626.

to be provided for a more accurate analysis.

In the exercise carried out for this application, it was thought worthwhile to order the candidate feeders for offering reactive support, based on the Lagrange multipliers provided as discussed in the previous Subsection. The ranking index proposed is the following:

$$n_i = w_p \Delta P_f \frac{P_{0,i}}{P_{0,f}} + w_q \Delta Q_f \frac{Q_{0,i}}{P_{0,f}} \quad (9)$$

where, ΔP_f is the change of the active power and ΔQ_f the change of the reactive power injected by the model test feeder for a specific control as in Section VI, while $P_{0,f}$ is the model test feeder active power injected at the base case and $P_{0,I}$, $Q_{0,I}$ is the injection of feeder i for the initial load flow (before contingency and load ramp). In Table 3 the chosen buses are presented.

The buses with the highest index are chosen to be equipped with ADN feeders and are shown in Table 5. The next step is to apply the distributed control scheme of Section IV.A to the selected feeders.

Three different controls are assumed for the DG converters: Constant (Tight) Voltage Control with the Voltage setpoint of the PVs equal to 1 p.u.; the same assuming LTC setpoint reduction to minimum; and CVC with DG buses at 1.05 pu (max permissible voltage) with LTC setpoint reduction.

In Table 6, the power exchange for each selected ADN feeder is shown after the control for each case. The distributed control is implemented only after the HV bus voltage is below 0.9 p.u.

As shown in Table 6, the active power for the first two control cases is not altered significantly as the generation remains constant and the voltage is set to 1 p.u.

In the maximum CVC case (1.05 pu), the voltage profile of the feeder is increased, meaning the loads will consume more power, thus increasing the active power flow to the distribution. In return, the reactive power generation of each DG is increased as seen in Fig. 11 (for one of the PVs connected in bus 1037) resulting in even greater reactive power flow to the transmission network until the power converter limits are met.

The effect of each control is observed in the simulated P-V curves for Peloponnese of Fig. 12, which is similar to Fig. 9, but is plotted for different control implementations. As seen in Fig. 12, the area

Table 5
Transmission support index for each feeder replaced.

Bus	P (MW)	Q (MVar)	wp	wq	Support index
626	28.840	6.040	0,2650	0,2573	3,2867
655	36.480	8.340	0,2514	0,1893	5,3422
673	32.420	5.670	0,2386	0,2211	4,0348
1037	36.350	14.380	0,2189	0,2416	6,0251
Total load	132.45	43.35	-	-	-

Table 6
Power exhange for constant active power for each feeder and control.

Bus	CVC ΔP_i	CVC ΔQ_i	CVC + LTC ΔP_i	CVC + LTC ΔQ_i	Max CVC + LTC ΔP_i	Max CVC + LTC ΔQ_i
626	0.409	-10.684	0.476	-25.355	6.519	-32.436
655	-0.754	-26.122	-0.583	-34.908	8.012	-54.140
673	1.035	-14.529	1.032	-30.728	8.078	-40.306
1037	0.050	-34.755	0.024	-38.582	7.984	-59.433

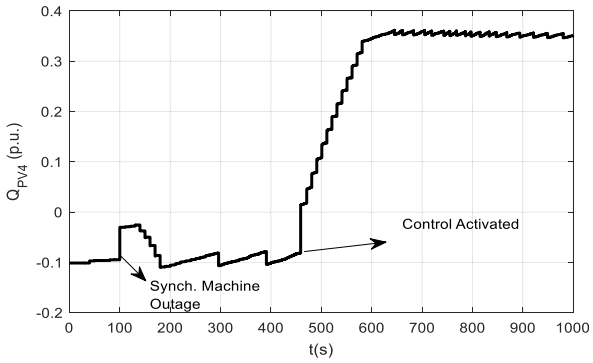

Fig. 11. Reactive power for one DG of feeder connected to bus 1037.

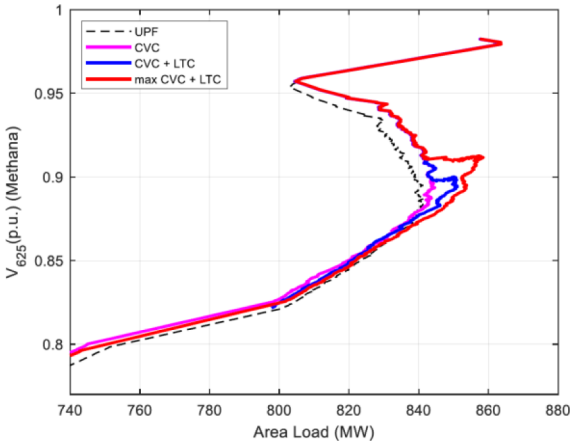

Fig. 12. P-V curve for Peloponnese for the three controls.

maximum consumption is increased by about 3.36 MW when DG buses are controlled to 1 pu, by 9.59 MW when the LTC setpoint is also changed and by about 17.04 MW when controlled to the maximum. It is noted that with the latter control the maximum consumption in Peloponnese becomes comparable with the pre-contingency load.

8. Conclusion

This paper proposes a distributed control scheme aiming to control active distribution networks in order to support the transmission system in terms of voltage stability margin.

The control scheme proposed was first examined in a small radial Transmission System connected with a test distribution feeder. The maximum and minimum active and reactive power injections are calculated and based on these the most effective way to increase the maximum loadability limit of the power system was examined. Three control strategies were followed, namely UPF, Q(V) control and Constant or Tight Voltage Control (CVC) by the DG converters. These controls were combined with LTC setpoint adjustments. Results proved that the maximum power transfer could be increased.

The proposed scheme was also used in the case of a historic voltage insecure snapshot of the Hellenic Interconnected System, assuming four

ADN feeders connected to important transmission buses. The results showed a quite important impact on voltage stability as measured by the increase of maximum power transfer into the affected area, proving that active distribution networks and DG placed in the MV network can contribute in terms of system voltage stability, if sufficient incentives are provided.

The requirements to achieve this type of control include special contracts with DG providers to participate in voltage stability support, as well as automation of LTC setpoint, both controlled by a distributed ADN feeder controller.

Declaration of Competing Interest

The authors declare that they have no known competing financial interests or personal relationships that could have appeared to influence the work reported in this paper.

References

[1] J.A. Pecas Lopes, N. Hatziargyriou, P.Djapic Mutale, K.J. Roesler, N. Jenkins, Integrating distributed generation into electric power systems: a review of drivers, challenges and opportunities, Electr. Power Syst. Res. (EPSR) 77 (Oct. 2007) 1189–1203.

[2] G. Valverde, T. Van Cutsem, Control of dispersed generation to regulate distribution and support transmission voltages, IEEE Grenoble Conference, June 2013, pp. 1–6.

[3] C. Vournas, I. Anagnostopoulos, T. Souxes, Transmission support using Wind Farm controls during voltage stability emergencies, Control Eng. Practice 59 (Feb. 2017) 100–110 G. O. Young, "Synthetic structure of industrial plastics," in *Plastics*, 2nd ed., vol. 3, J. Peters, Ed. New York: McGraw-Hill, 1964, pp. 15-64.

[4] N. Hatziargyriou, et. al., Contribution to bulk system control and stability by distributed energy resources connected at distribution network, IEEE Power & Energy Soc. (Jan. 2017) Tech. Rep. PES-TR22.

[5] D. Mayorga Gonzalez, L. Robitzky, S. Liemann, U. Hager, J. Myrzik, C. Rehtanz, Distribution network control scheme for power flow regulation at the interconnection point between transmission and distribution system, IEEE Innovative Smart Grid Technologies - Asia (ISGT-Asia), IEEE, 2016, pp. 23–28 2016.

[6] P. Aristidou, G. Valverde, T. Van Cutsem, Contribution of distribution network control to voltage stability: a case study, IEEE Trans. Smart Grid. 8 (1) (Jan. 2017) 106–116.

[7] L. Aolaritei, S. Bolognani, F. Dörfler, Hierarchical and distributed monitoring of voltage stability in distribution networks, IEEE Trans. Power Syst. 33 (6) (Nov. 2018) 6705–6714.

[8] Z.S. Li, Q.L. Guo, H.B. Sun, J.H. Wang, Y.L. Xu, M. Fan, A distributed transmission-distribution-coupled static voltage stability assessment method considering distributed generation, IEEE Trans. Power Syst. 33 (3) (May 2018) 3621–3632.

[9] V. Calderaro, V. Galdi, F. Lamberti, A. Piccolo, 'Optimal decentralized voltage control for distributed systems with inverter-based distributed generators, IEEE Trans. Power Syst 29 (1) (2014) 230–241.

[10] S. Weckx, J. Driesen, Optimal local reactive power control by PV inverters, IEEE Trans. Sustain. Energy 7 (4) (Oct. 2016) 1624–1633.

[11] J. Buire, F. Colas, J. Dieulot, L. de Alvaro, X. Guillaud, Confidence level optimization of dg piecewise affine controllers in distribution grids, IEEE Trans. Smart Grid. (2019).

[12] V. Zamani, M.E. Baran, Meter placement for conservation voltage reduction in distribution systems, IEEE Trans. Power Syst. 33 (2) (March 2018) 2109–2116.

[13] T. Van Cutsem, C. Vournas, Voltage Stability of Electric Power Systems, Springer, 2008.

[14] S.C. Savulescu, Real-time stability in power systems: techniques for early detection of the risk of blackout, Power Electronics and Power Systems, 2nd edition, Springer International Publishing, Cham, 2014.

[15] T. Van Cutsem, J. Kabouris, G. Christoforidis, C. Vournas, Application of real-time voltage security assessment to the Hellenic interconnected system, IEE Proceedings - Generation, Transmission and Distribution, 152 Jan. 2005, pp. 123–131.